Electronic Supplementary Information

P=P Bond Photophysics in an Ar-P=P-Ar Diphosphene

Huo-Lei Peng, John L. Payton, John D. Protasiewicz, M. Cather Simpson

Full references for Gaussian and MolPro.

(9) Werner, H.-J.; P.J. Knowles; Lindh, R.; Manby, F. R.; Schütz, M.; Celani, P.; Korona, T.; Mitrushenkov, A.; Rauhut, G.; Adler, T. B.; Amos, R. D.; Bernhardsson, A.; Berning, A.; Cooper, D. L.; Deegan, M. J. O.; Dobbyn, A. J.; Eckert, F.; Goll, E.; Hampel, C.; Hetzer, G.; Hrenar, T.; Knizia, G.; Köppl, C.; Liu, Y.; Lloyd, A. W.; Mata, R. A.; May, A. J.; McNicholas, S. J.; Meyer, W.; Mura, M. E.; Nicklass, A.; Palmieri, P.; Pflüger, K.; Pitzer, R.; Reiher, M.; Shumann, U.; Stoll, H.; Stone, A. J.; Tarroni, R.; Thorsteinsson, T.; Want, M.; Wolf, A., MolPro 2006.1 **2006**

(12) Frisch, M. J.; Trucks, G. W.; Schlegel, H. B.; G. E. Scuseria, M. A. R., J. R. Cheeseman, J. A. Montgomery, Jr., T. Vreven, K. N. Kudin, J. C. Burant, J. M. Millam, S. S. Iyengar, J. Tomasi, V. Barone, B. Mennucci, M. Cossi, G. Scalmani, N. Rega, G. A. Petersson, H. Nakatsuji, M. Hada, M. Ehara, K. Toyota, R. Fukuda, J. Hasegawa, M. Ishida, T. Nakajima, Y. Honda, O. Kitao, H. Nakai, M. Klene, X. Li, J. E. Knox, H. P. Hratchian, J. B. Cross, C. Adamo, J. Jaramillo, R. Gomperts, R. E. Stratmann, O. Yazyev, A. J. Austin, R. Cammi, C. Pomelli, J. W. Ochterski, P. Y. Ayala, K. Morokuma, G. A. Voth, P. Salvador, J. J. Dannenberg, V. G. Zakrzewski, S. Dapprich, A. D. Daniels, M. C. Strain, O. Farkas, D. K. Malick, A. D. Rabuck, K. Raghavachari, J. B. Foresman, J. V. Ortiz, Q. Cui, A. G. Baboul, S. Clifford, J. Cioslowski, B. B. Stefanov, G. Liu, A. Liashenko, P. Piskorz, I. Komaromi, R. L. Martin, D. J. Fox, T. Keith, M. A. Al-Laham, C. Y. Peng, A. Nanayakkara, M. Challacombe, P. M. W. Gill, B. Johnson, W. Chen, M. W. Wong, C. Gonzalez, and J. A. Pople, Gaussian 03 (Revision D.01) **2003.**

Computational Details – the Active Space; The Geometry Definitions.

Geometry optimizations of 1,2-*bis*(phenyl)diphosphene (PhP=PPh) were performed using the complete active space self-consistent field (CASSCF) approach with a 6-31G** basis set. The energies of selected points were calculated using second order perturbation theory (CASPT2). An active space of eight electrons and six orbitals, (8/6), consisting of the phosphorous based σ_{PP}, n_-, n_+, π_{PP}, π_{PP}*, and σ_{PP}* orbitals (Figure S1), was chosen as a compromise between accuracy and computational expense.

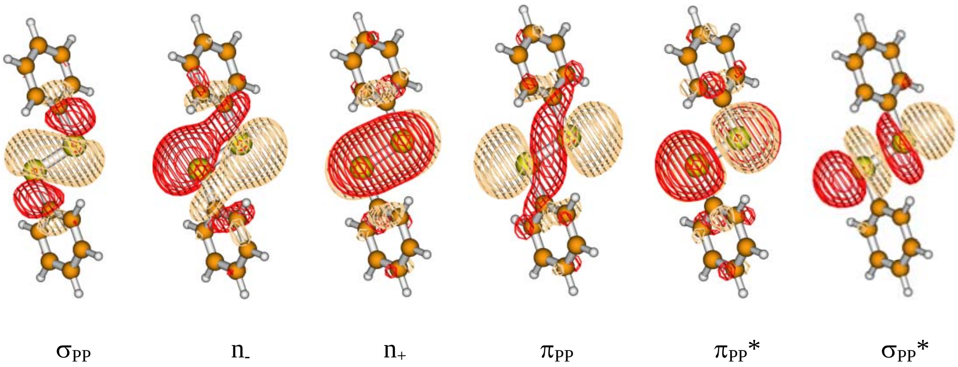
σ_{PP} n_- n_+ π_{PP} π_{PP}* σ_{PP}*

Figure S1. The (8/6) active space orbitals plotted with an isovalue of 0.02.

B3LYP/3-21G(d) and B3LYP/6-31+G(d,p)//3-21G(d) were used to estimate the barrier to torsional rotation about the bonds between the phenyl rings and phosphorus atoms (α_1 and α_2), and the barrier to torsional rotation about the central C-P=P-C unit (τ) (Figure S2) This was accomplished through geometry optimizations with constraints along these coordinates.

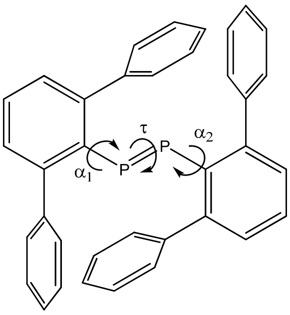

Figure S2. Definition of the the phenyl twist angles α_1 and α_2 and the C-P=P-C torsion angle τ.

The B3LYP hybrid functional has proven to be a versatile functional suitable for most of the ground state energy excitations and perturbations calculated in this paper. Unfortunately, it performs rather poorly near the transition state for the τ rotation coordinate about the P=P bond, and may overestimate the actual ground state *trans*-to-*cis* rotation barrier by as much as 50%.[34]

Computational Results.

- Geometries calculated at the CASSCF/6-31G** level.

Table S1. Summary of important geometric parameters for PhP=PPh

State	**P=P (A)**	**P-C (A)**	**P=P-C (°)**	**$\alpha_1 = \alpha_2$ (°)**	**τ (°)[a]**
S_0	2.091	1.845	101	50	177[b]
S_0	2.092	1.846	101	53	180
S_1 ($n_+\pi^*$)	2.184	1.826	109	91	180
S_2 ($\pi\pi^*$)	2.349	1.795	101	0.1	180
T_1 ($\pi\pi^*$)	2.344	1.827	101	0.2	180
T_2 ($n_+\pi^*$)	2.179	1.832	108	92	180

a. Geometry optimizations constrained along this coordinate at τ = 180°, except where indicated.
b. Full, unconstrained geometry optimization.

S_0 state – unconstrained *trans*- conformation

	X	Y	Z
P	0.00000000	0.00000000	0.00000000
P	0.00000000	0.00000000	2.09104923
C	0.00000000	1.81000703	2.44631900
C	-0.09855166	-1.80713169	-0.35608662
C	0.77801867	-2.31921598	-1.31102704
C	0.74458899	-3.65874194	-1.65960804
C	-0.17843640	-4.50561757	-1.06851091
C	-1.06677581	-4.00674323	-0.13058933
C	-1.02956115	-2.66758630	0.22199280
C	0.90587911	2.27504618	3.39796819
C	0.94533761	3.61466659	3.74550510
C	0.06703081	4.50936409	3.15668514
C	-0.84982785	4.05814236	2.22210374
C	-0.88549336	2.71866277	1.87051928
H	1.49437433	-1.66931118	-1.78370078
H	1.43441448	-4.03802950	-2.39273240
H	-0.20971078	-5.54553015	-1.34198980
H	-1.79145504	-4.65766130	0.32590919
H	-1.73208062	-2.29489157	0.94513231
H	1.58798817	1.58804895	3.86884122
H	1.65688350	3.95698058	4.47606311
H	0.09237468	5.54963897	3.42939744
H	-1.54010477	4.74662072	1.76739401
H	-1.60929526	2.38358890	1.14995480

S_0 state – constrained to the *trans*-conformation $\tau = 180°$

	X	Y	Z
P	0.00000000	0.00000000	0.00000000
P	0.00000000	0.00000000	2.09206549
C	0.00000000	1.81172913	2.44564694
C	0.00000000	-1.81172983	-0.35357838
C	-0.91598589	-2.71173500	0.18602613
C	-0.87467054	-4.05264480	-0.15950755
C	0.07846770	-4.51316385	-1.05237151
C	0.98734870	-3.62636017	-1.60508552
C	0.94247741	-2.28498444	-1.26365402
C	-0.91597269	2.71174018	1.90602969
C	-0.87465636	4.05264884	2.25156738
C	0.07846961	4.51316112	3.14444805
C	0.98733693	3.62635166	3.69717507
C	0.94246452	2.28497693	3.35573949
H	-1.66703482	-2.36908588	0.87471659
H	-1.58842741	-4.73498448	0.26738450
H	0.10849349	-5.55448476	-1.32055078
H	1.72735889	-3.97568822	-2.30335432
H	1.64909433	-1.60439393	-1.70690751
H	-1.66701205	2.36909669	1.21732600
H	-1.58840278	4.73499310	1.82466517
H	0.10849572	5.55448113	3.41263077
H	1.72733729	3.97567435	4.39545696
H	1.64907065	1.60438178	3.79900304

S_1 state – constrained to the *trans*-conformation τ = 180°

	X	Y	Z
P	0.00000000	0.00000000	0.00000000
P	0.00000000	0.00000000	2.18441867
C	0.00000000	1.72477304	2.78327330
C	0.00000000	-1.72477307	-0.59885459
C	1.20112780	-2.38667874	-0.85942447
C	1.20088037	-3.67980319	-1.35266609
C	0.00000551	-4.32642428	-1.59891364
C	-1.20087832	-3.67979852	-1.35269184
C	-1.20112820	-2.38668334	-0.85943582
C	1.20112781	2.38667884	3.04384288
C	1.20088040	3.67980328	3.53708454
C	0.00000554	4.32642422	3.78333244
C	-1.20087829	3.67979833	3.53711095
C	-1.20112820	2.38668318	3.04385487
H	2.13369555	-1.88699330	-0.67019387
H	2.13329918	-4.18041254	-1.54454240
H	0.00002047	-5.33123695	-1.98346573
H	-2.13329831	-4.18041115	-1.54454993
H	-2.13369549	-1.88701206	-0.67016490
H	2.13369553	1.88699348	2.85461200
H	2.13329921	4.18041273	3.72896060
H	0.00002046	5.33123687	4.16788459
H	-2.13329827	4.18041086	3.72896931
H	-2.13369550	1.88701184	2.85458417

S_2 state – constrained to the *trans*-conformation τ = 180°

	X	Y	Z
P	0.00000000	0.00000000	0.00000000
P	0.00000000	0.00000000	2.34910096
C	0.00000000	1.76398725	2.67933128
C	0.00000000	-1.76400162	-0.33017326
C	-0.00145827	-2.11745520	-1.69533293
C	-0.00169406	-3.43483997	-2.09613009
C	-0.00045735	-4.44955149	-1.14606765
C	0.00105128	-4.13028428	0.20113099
C	0.00128741	-2.80820644	0.60892664
C	0.00144861	2.11740196	4.04449793
C	0.00167334	3.43477757	4.44533620
C	0.00036114	4.44951311	3.49530474
C	-0.00119642	4.13028337	2.14809332
C	-0.00138010	2.80822222	1.74025954
H	-0.00239540	-1.33976976	-2.43925849
H	-0.00285293	-3.67634412	-3.14415622
H	-0.00064895	-5.47925344	-1.45692422
H	0.00211064	-4.91251029	0.93936772
H	0.00255050	-2.59432303	1.65949312
H	0.00252132	1.33969570	4.78840181
H	0.00285244	3.67624530	5.49337043
H	0.00053073	5.47920886	3.80618199
H	-0.00222578	4.91253507	1.40988368
H	-0.00271435	2.59436613	0.68968752

T_1 state – constrained to the *trans*-conformation τ = 180°

	X	Y	Z
P	0.00000000	0.00000000	0.00000000
P	0.00000000	0.00000000	2.34362421
C	0.00000000	1.79212891	2.70143074
C	0.00000000	-1.79207381	-0.35809013
C	-0.00306224	-2.12346046	-1.71834446
C	-0.00319079	-3.44109610	-2.13449213
C	-0.00018248	-4.46251286	-1.19706188
C	0.00295350	-4.15490505	0.15269495
C	0.00304616	-2.83437283	0.57088262
C	0.00426141	2.12372369	4.06163126
C	0.00441717	3.44142332	4.47757612
C	0.00021408	4.46269536	3.53999257
C	-0.00414012	4.15488012	2.19028630
C	-0.00424800	2.83428364	1.77230203
H	-0.00540059	-1.33864000	-2.45526046
H	-0.00562220	-3.67071939	-3.18535255
H	-0.00027149	-5.48957434	-1.51702074
H	0.00533101	-4.94285820	0.88504381
H	0.00555664	-2.62840065	1.62405737
H	0.00752333	1.33901617	4.79866445
H	0.00779692	3.67120955	5.52839829
H	0.00032280	5.48980571	3.85979441
H	-0.00745855	4.94272032	1.45781960
H	-0.00772827	2.62814698	0.71916168

T_2 state – constrained to the *trans*-conformation τ = 180°

	X	Y	Z
P	0.00000000	0.00000000	0.00000000
P	0.00000000	0.00000000	2.17893131
C	0.00000000	1.73888090	2.75512657
C	0.00000000	-1.73888844	-0.57619106
C	-1.20020494	-2.40152080	-0.82994444
C	-1.20045496	-3.69815117	-1.31555632
C	-0.00000712	-4.34594132	-1.55876778
C	1.20044937	-3.69737757	-1.31762022
C	1.20020118	-2.40076635	-0.83197717
C	1.20024060	2.40167690	3.00841449
C	1.20051539	3.69829321	3.49399863
C	0.00006287	4.34593559	3.73771005
C	-1.20038604	3.69722396	3.49705712
C	-1.20016151	2.40059468	3.01139589
H	-2.13295621	-1.90101301	-0.64303109
H	-2.13305995	-4.19986753	-1.50374943
H	-0.00001042	-5.35315264	-1.93707589
H	2.13304789	-4.19847690	-1.50748113
H	2.13294060	-1.89966444	-0.64659976
H	2.13297205	1.90126989	2.82113512
H	2.13312356	4.20014519	3.68181373
H	0.00010786	5.35314369	4.11602688
H	-2.13298645	4.19817512	3.68729843
H	-2.13292479	1.89940494	2.82637205

- Energies from CASSCF(8,6)/6-31G** and CASPT2(8,6)/6-31G**//CASSCF(8,6)/6-31G** computational levels for the ground and excited states reported in this manuscript.

Table S2. Summary of absolute energies for the geometry optimized states of PhP=PPh.

State	**CASSCF** **E (hartree)**	**CASPT2//CASSCF** **E (hartree)**	**constrained to τ = 180°**
S_0	-1141.725753	-1143.453505	N[a]
S_0	-1141.725631	-1143.453323	Y
S_1 ($n_+\pi^*$)	-1141.618760	-1143.353801	Y
S_2 ($\pi\pi^*$)	-1141.568416	[a]	Y
T_1 ($\pi\pi^*$)	-1141.666971	-1143.401158	Y
T_2 ($n_+\pi^*$)	-1141.639389	-1143.378473	Y

a. Full, unconstrained geometry optimization.

- Vertical transition (excitation and de-excitation) energies and oscillator strengths calculated at the CASSCF(8,6)/6-31G** and CASPT2(8,6)/6-31G**//CASSCF(8,6)/6-31G** levels. All optimizations were performed under the single constraint of τ = 180° to prevent relaxation along this coordinate.

Table S3. Transition energies and oscillator strengths from the S_0 (τ=180°) geometry

	CASSCF			**CASPT2//CASSCF**	
	ΔE (eV)	**λ (nm)**	***f***	**ΔE (eV)**	**λ (nm)**
$S_1(n_+\pi^*) \leftarrow S_0$	3.253	381	0.0083	2.856	434
$S_2(\pi\pi^*) \leftarrow S_0$	5.196	239	0.1734	4.189	296
$S_3(n_-\pi^*) \leftarrow S_0$	5.089	244	0.0948	4.255	291
$S_4(\pi^0\pi^{*2}) \leftarrow S_0$	6.649	187	0.0016	6.247	199

Table S4. Transition energies and oscillator strengths from the S_1 (τ=180°) geometry

	CASSCF			**CASPT2//CASSCF**	
	ΔE (eV)	**λ (nm)**	***f***	**ΔE (eV)**	**λ (nm)**
$S_1(n_+\pi^*) \rightarrow S_0$	-2.566	(-)483	0.0000	-2.179	(-)569
$S_2(\pi\pi^*) \leftarrow S_1(n_+\pi^*)$	2.562	484	0.0003	2.786	445
$S_3(n_-\pi^*) \leftarrow S_1(n_+\pi^*)$	1.899	653	0.0019	1.513	820
$S_4(\pi^0\pi^{*2}) \leftarrow S_1(n_+\pi^*)$	2.729	454	0.0000	2.786	445

Table S5. Transition energies and oscillator strengths from the S_2 (τ=180°) geometry

	CASSCF			**CASPT2//CASSCF**^{a}	
	ΔE (eV)	**λ (nm)**	***f***	**ΔE (eV)**	**λ (nm)**
$S_2(\pi\pi^*) \rightarrow S_0$	-3.660	(-)339	0.1369		
$S_2(\pi\pi^*) \rightarrow S_1(n_+\pi^*)$	-0.603	(-)2057	0.0001		
$S_3(n_-\pi^*) \leftarrow S_2(\pi\pi^*)$	0.711	1744	0.000		
$S_4(\pi^0\pi^{*2}) \leftarrow S_2(\pi\pi^*)$	0.993	1248	0.1635		

a. We were unable to get the CASPT2 calculations for the $S_2(\pi\pi^*)$ constrained (τ = 180°) geometry to converge properly; further calculations to resolve this issue will be taken in future.

Table S6. Transition energies and oscillator strengths from the T_1 (τ=180°) geometry

	CASSCF			**CASPT2//CASSCF**	
	ΔE (eV)	**λ (nm)**	***f***	**ΔE (eV)**	**λ (nm)**
$T_2(n_+\pi^*) \leftarrow T_1(\pi\pi^*)$	1.363	910	0.0067	1.267	978
$T_3(n_-\pi^*) \leftarrow T_1(\pi\pi^*)$	3.263	380	0.0000	2.953	420
$T_4(n_+\sigma^*) \leftarrow T_1(\pi\pi^*)$	3.811	325	0.0000	3.503	354
$T_5(\pi\sigma^*) \leftarrow T_1(\pi\pi^*)$	3.819	325	0.0018	3.512	353

Table S7. Transition energies and oscillator strengths from the T_2 (τ=180°) geometry

	CASSCF			**CASPT2//CASSCF**	
	ΔE (eV)	**λ (nm)**	***f***	**ΔE (eV)**	**λ (nm)**
$T_2(n_+\pi^*) \rightarrow T_1(\pi\pi^*)$	-0.188	(-)6579	0.0011	0.075	16461
$T_3(n_-\pi^*) \leftarrow T_2(n_+\pi^*)$	2.267	547	0.0091	2.111	587
$T_4(n_+\sigma^*) \leftarrow T_2(n_+\pi^*)$	3.267	380	0.0004	2.848	435
$T_5(n_+{}^1\pi^1\pi^{*2}) \leftarrow T_2(n_+\pi^*)$	3.528	352	0.1439	2.987	415

- DFT computations upon the full DmpP=PDmp compound. See Figure S2 for definitions of degrees of freedom.

Rotation about the P=P bond. The thermal (ground state) barrier to rotation about the central P=P bond (τ) is 52.6 kcal/mol at the B3LYP/6-31+G**//3-21G* level for DmpP=PDmp. The rotation transition state occurs at ~100° rather than at the midpoint of 90°, most likely due to errors associated with the single-determinant DFT method around the transition state. CAS calculations indicate that more than one determinant is needed to accurately describe the region around the τ = 90° geometry.

Twisting about the P-phenyl bonds. When one phenyl-PP torsion angle is constrained and the remainder of the molecule allowed to geometrically relax (red traces, Figure S3), the other ligand rotates in concert with ease ($\alpha_1 = -\alpha_2 + 108^o$; $r^2 = 0.99$) to keep the two phenyl rings at a nearly constant 77 ± 2^o relative to one another. The energy changes by < 2 kcal/mol across the entire range of phenyl twist angles. This low-barrier motion is reflected in the crystal structure of DmpP=PDmp, in which the two phenyl twist angles are 81^o and 13° (ref. 3) and the large variety of phenyl twist angles, and crystal structure disorder, observed in the crystal structures of many aryl diphosphenes.[43] Forcing the twist angles to be equal (*i.e.* $\alpha_1 = \alpha_2$) leads to slightly higher barriers at 11.6 kcal/mol (rings coplanar with P=P) and 4.0 kcal/mol (rings perpendicular to P=P) (blue traces, Figure S3). Thus the central P=P appears to be able to freely swivel about inside the "cocoon" of the Dmp ligands, without adopting a *cis*-conformation.

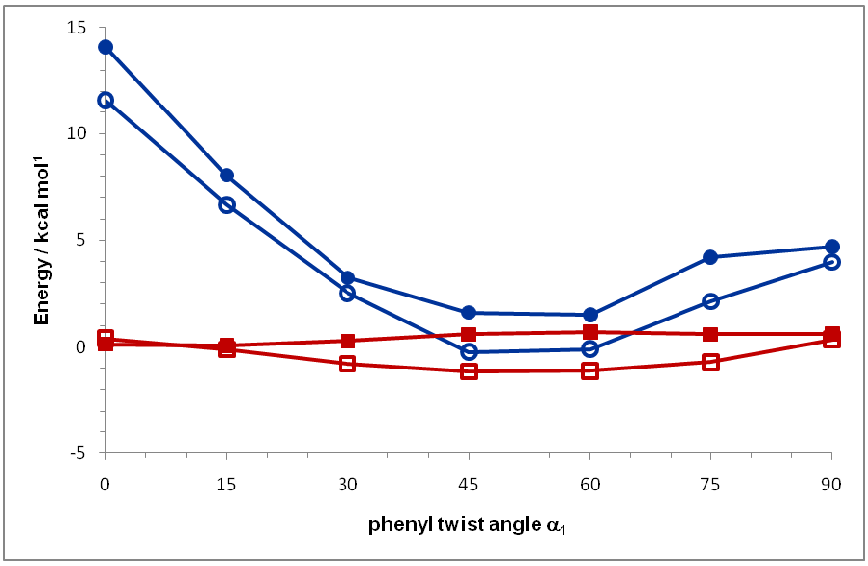

Figure S3. The ground state potential energy surface associated with the diagonal $\alpha_1 = \alpha_2$ (blue circles) and single α_1 only (red squares) phenyl twist angle distortions of *trans*-DmpP=PDmp. Calculated at the B3LYP/3-21G* (filled symbols) and B3LYP/6-31+G**//3-21G* levels.

- Quenching of 2,3-butanedione phosphorescence with DmpP=PDmp. This molecule was chosen because it has a high triplet quantum yield with phosphorescence observable at room temperature,[1] and the energy of its lowest triplet state is 55 kcal/mol,[2-6] higher than that of DmpP=PDmp. Excitation of the singlet diketone leads to triplet-triplet energy transfer to the low-lying DmpP=PDmp triplet states (right panel, Figure S4).

The DmpP=PDmp / diketone quenching experiments were performed as follows. Cyclohexane and diketone (2,3-butanedione) were distilled before use. Solutions of 0.01 M diketone in cyclohexane were subjected to three cycles of freeze-pump-thaw to ensure an oxygen-free solution. Freezing was accomplished with an ice-NaCl bath (T < 10°C). The DmpP=PDmp concentration was set to 0.2 mM for quenching experiments. UV-Vis absorption measurements were carried out on a Cary 100 spectrometer; fluorescence (not shown) and phosphorescence measurements were performed on a Cary 5 spectrometer. For phosphorescence measurements, the delay time was set to 0.1 ms and the gate to 1.0 ms. All measurements were performed at room temperature.

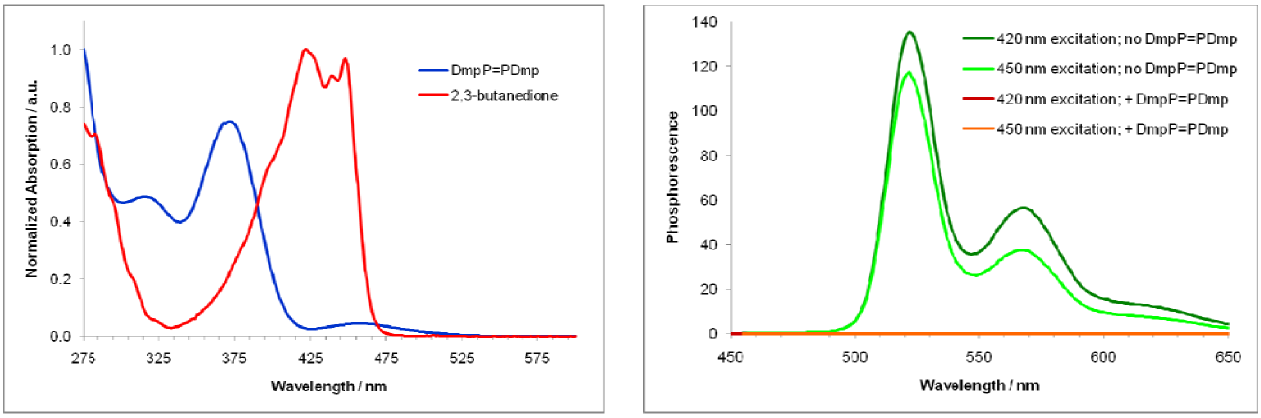

Figure S4. Left panel: Normalized UV/Vis absorption spectra of DmpP=PDmp in cyclohexane (blue) and 2,3-butanedione in cyclohexane (red). Right panel: Phosphorescence from 0.01 M 2,3-butanedione in cyclohexane excited at 420 nm without DmpP=PDmp (dark green) and with 0.2 mM DmpP=PDmp (dark orange). Excitation at 450 nm without DmpP=PDmp (light green) and with 0.2 mM DmpP=PDmp (light orange). All experiments performed under anaerobic conditions at room temperature.

Supporting Information References

1. Y. Tsuboi, K. Okada, S. Ishizaka and N. Kitamura, *Analytical Sciences*, 2005, **21**, 303-308.
2. C. C. Wamser, R. T. Medary, I. E. Kochevar, N. J. Turro and P. L. Chang, *J. Am. Chem. Soc.*, 1975, **97**, 4864-4869.
3. J. C. D. Brand and A. W. H. Mau, *J. Am. Chem. Soc.*, 1974, **96**, 4380-4385.
4. H. W. Sidebottom, C. C. Badcock, J. G. Calvert, B. R. Rabe and E. K. Damon, *J. Am. Chem. Soc.*, 1972, **94**, 13-19.
5. N. J. Turro and R. Engel, *J. Am. Chem. Soc.*, 1969, **91**, 7113-7121.
6. T. R. Evans and P. A. Leermakers, *J. Am. Chem. Soc.*, 1967, **89**, 4380-4382.